

Investigating the Adhesive Wear Properties of Aluminum Hybrid Metal Matrix Composites at Elevated Temperatures Using RSM Technique

C. Aravind^a, S. Gopalakrishnan^a, N. Radhika^{a,*}

^aDepartment of Mechanical Engineering, Amrita School of Engineering, Coimbatore, Amrita Vishwa Vidyapeetham, India.

Keywords:

Adhesive wear
Hybrid Metal Matrix Composite
Elevated temperature
Scanning electron microscope
Response Surface Methodology

ABSTRACT

Fabrication of Aluminum LM13/MoS₂/TiO₂ hybrid metal matrix composite via stir casting technique was carried out to analyze the wear characteristics at an elevated temperature of 150° C using pin on disc tribometer. The parameters namely load, sliding velocity and sliding distance were varied for five levels as per the run order generated from Response Surface Methodology. From experiments, it was observed that the wear rate decreased with reduced sliding velocity initially due to mechanically mixed layer formation and then increases. Also the results showed a reduction in wear rate with low loading and sliding distance conditions. Minimum wear rate was observed at a load of (11N), sliding velocity (1m/s) and sliding distance (848m) which was the ideal condition. Results concluded that the load applied was the significant factor over rate of wear leading to the occurrence of deep grooves along with delamination at higher loads. At minimal loads, appearance of shallow grooves in the sliding direction was observed. Major Applications of AMMC include the manufacturing of piston liners in automobiles and bearings, gears for aircraft engines which are often subjected to high friction and temperatures.

* Corresponding author:

N. Radhika 
E-mail: n_radhika1@cb.amrita.edu

Received: 29 April 2019
Revised: 27 June 2019
Accepted: 11 August 2019

© 2019 Published by Faculty of Engineering

1. INTRODUCTION

Metal Matrix Composites (MMCs) was a significant candidate of material system as there had been a constant requirement for it to meet various global demands. Unlike monolithic materials, these MMCs can be custom tailored by adding reinforcements to the base metal. Aluminum metal matrix composite (AMMC) refers to a class of lightweight, cost effective and

high performance material which has significant characteristics namely lower coefficient of thermal expansion, higher strength-weight ratios and excellent wear resistance [1]. They are being widely used in automotive applications like bearing surfaces, cylinder liners, pistons, camshafts, rockers and brake components [2-3]. Researchers have studied various tribological properties of particulate reinforced MMCs [4]. Idrisi and Deva studied

AMMCs reinforced with SiC (0%, 3%, 5%, 8%, 10%wt) particles fabricated using ultrasonic assisted stir casting method and concluded that mechanical properties had improved significantly with rise in 10wt% of SiC particles [5]. Sumod et al. fabricated LM13 alloy with Nano ZrO₂ reinforcement using stir casting technique and indicated increased rate of hardness with increased quantity of Nano ZrO₂ particles and also observed reduced thermal conductivity [6]. Kannappan et al. perceived that wear resistance of Al-Si10Mg/2wt% MoS₂ composite fabricated via stir casting route increased by 55 % compared with the unreinforced alloy at room temperature condition [7]. David et al. confirmed an increase in wear resistance of Al-SiC (7.5,10wt%)/ fly ash (7.5wt%) hybrid composite fabricated via liquid metallurgy route, where a high dislocation density due to thermal mismatch was observed when more than one reinforcement was added at room temperature [8]. Hariprasad et al. observed that hybrid composite Al-Al₂O₃ (0.5wt %) / B₄C (0%, 3%, 5%wt) fabricated via stir casting showed that a increased weight percent of B₄C content improved the respective wear characteristic [9]. Sharma et al. investigated the wear properties of Al6016-garnet particulate (8 and 12wt%) reinforced composites and showed an improvement compared to that of unreinforced alloy [10]. Mehtap et al. explained that sliding wear characteristic of Aluminum/Ni₃Al composite varied significantly with temperature and load and observed that the decreased weight percent of Ni₃Al reinforcements led to rise in rate of wear [11]. Asif et al. investigated Al-20SiCp composite with (hybrid) and without (binary)solid lubricants namely graphite and Sb₂S₃). The analysis indicated that rate of wear of binary composite was higher than hybrid composite [12].

Optimization techniques such as Response surface methodology (RSM) and Taguchi method have become a major part in research and development process in the recent years. Sharma et al. fabricated Aluminum 6061 hybrid MMC reinforced with Si₃N₄ (3-6wt%) / Nano graphite powder (3-15wt%)[13]. Similarly, researchers Bayhan and Onel fabricated Al-Si7Mg/SiC composite, analyzed using RSM and revealed that increase in reinforcement weight

% favored minimization of wear rate [14]. Prasat et al. fabricated AlSi10Mg/Fly ash (9wt%)/ Graphite (3wt%) composite through liquid metallurgy route and optimized using Taguchi method and observed that rate of wear was most affected by sliding distance parameter [15], while researcher Radhika et al fabricated and analyzed aluminum alloy reinforced with alumina (6wt%)/Graphite(3wt%) using the same technique and determined that the effect of load had highest effect on rate of wear [16].

The literature review provided an understanding that numerous research work have been carried out in determining the wear properties of hybrid MMC at room temperature conditions, however studies involving determination of wear behavior of MMCs at elevated temperatures have not been fully explored. Therefore, the aim of this research work is to analyze the behavior of wear characteristics of fabricated LM13/TiO₂/MoS₂ hybrid composite at an elevated temperature. RSM is employed to analyze the wear characteristics.

2. MATERIAL SELECTION AND FABRICATION METHOD

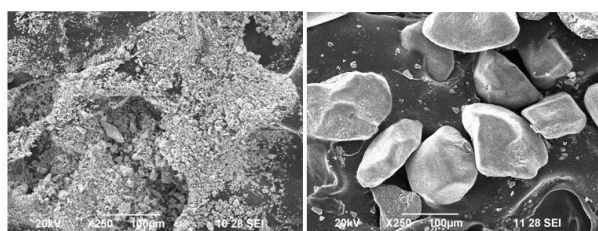
The characteristic of a composite material is determined by the selection of appropriate reinforcements and base matrix. In the present investigation, LM13 (Eutectic alloy) with density of 2.7g/cm³ was chosen as a base metal matrix. The elemental composition of LM13 alloy is shown in Table 1. The mechanical and thermal properties improve by incorporating reinforcements in the base matrix [17]. The reinforcements added were 3 wt% of Molybdenum disulphide(MoS₂) with average grain size of 10µm (Fig. 1a) and 12 wt% of Titanium dioxides(TiO₂) with average grain size of 30µm (Fig. 1b) with densities of 5.06g/cm³ and 4.23g/cm³ respectively. The calculated density of HMMC was determined using the rule of mixtures given by (1):

$$\rho_c = \text{wt. m} \times \rho_m + \text{wt. a} \times \rho_a + \text{wt. b} \times \rho_b \quad (1)$$

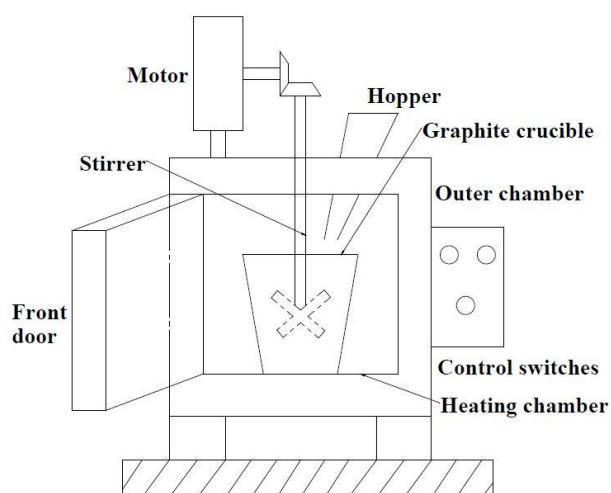
where ρ_c , ρ_m , ρ_a and ρ_b are the densities of the Hybrid MMC, LM13 matrix, MoS₂ and TiO₂ respectively while wt. m, wt. a and wt. b, are weight fractions of LM13 matrix, MoS₂ and TiO₂ respectively.

Table 1. Elemental Composition of LM13 Alloy.

Elemental Composition	Wt % (max)
Cu	1.5
Mg	1.5
Si	13.0
Fe	1.0
Mn	0.5
Ni	1.5
Zn	0.5
Pb	0.1
Ti	0.2
Sn	0.1
Al	Remainder

(a) MoS₂(b) TiO₂**Fig. 1.** Microstructure of reinforcements.

MoS₂ has a direct impact over wear rate as it possesses good self-lubricating property which is comparable to that of graphene. The distinctive feature is that, it is also used in vacuum conditions [18]. The excellent mechanical properties of TiO₂ (good strength and thermal conductivity) allows it to be used in regions of high temperatures.

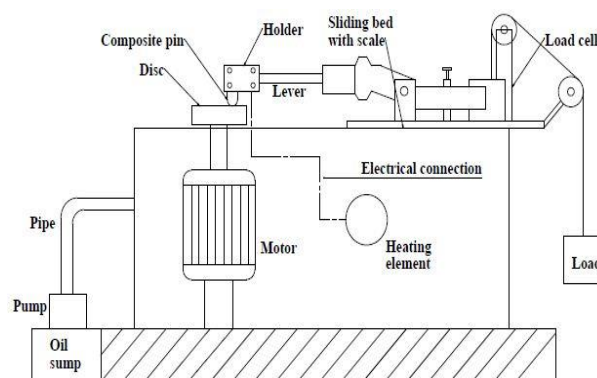
**Fig. 2.** Schematic representation of electrical furnace with stirrer.

A simple and cost-effective method (Liquid metallurgy-based stir casting) was chosen in this work. Initially, LM13 Al ingot alloy was loaded into a graphite crucible and heated in an electric furnace at 760 °C under argon

atmosphere (Fig. 2). The reinforcements MoS₂ and TiO₂ were preheated (350 °C) initially as it reduces the temperature gradient between the matrix and reinforcement and removes moisture leading to increase in wettability. These reinforcements were introduced into the melt and stirred for 10 minutes using a mechanical stirrer at a speed of 250 rpm to attain uniform distribution. A stainless-steel die of diameter 20 mm and length 150 mm was used to solidify the melt.

2.1 Adhesive Wear Test

Dry sliding wear characteristics of hybrid composite at an elevated temperature was determined using a pin on disc tribometer (DUCOM-HRC 65) (Fig. 3).

**Fig. 3.** Representation of Pin on disc tribometer.**Fig. 4.** Cylindrical hybrid composite pins.

From the cast specimen, pins of size 14 mm diameter and length of 35 mm were machined (Fig. 4). As per ASTM G99 standards, experiments were performed under dry and non-abrasive conditions at a high temperature (150 °C). Emery paper was used in polishing the rotating EN32 steel disc (with an elemental composition of C (0.18 %), Mn (1 %), Si (0.35 %), P (0.05 %), S (0.05 %)); and 8 mm thickness) before the initiation of each experiment for removing debris. The composite pin was

thoroughly cleaned using acetone solution and checked for surface imperfections and was weighed accurately using a weighing machine of least count 0.0001 g. The composite pin was then heated to 150 °C using a heating element. On initiation of the test, the pin was held pressed on the hardened counter face and a load was applied which acted as a counter weight and balanced the pin. The specimen for each cycle followed a constant track diameter of 80 mm. On completing each experiment, the composite pin was removed, cooled to room temperature with external forced convection and cleaned from debris before reweighing it to determine the mass loss. The mass loss (Δm) was determined from the difference (Initial and Final weights) in weights of the composite specimen occurred due to wear. Using the equation (2) the volumetric rate of wear was calculated:

$$W = \Delta m / (\rho \times D) \quad (2)$$

where ρ -density (g/mm^3), W - wear rate (mm^3/m), Δm -mass loss (g) and D -sliding distance (m) of the hybrid composite specimen.

2.2 Response Surface Methodology

RSM involves developing a model with aid of statistical methods and analyzing the problems where multiple parameters influence the response of unique interest. The purpose of this method was in optimizing that response. RSM provides a large amount of information with a minimal amount of experimentation; hence it was a promising analytical tool to predict the response of parameters [19]. This method was adopted here to study the relationship between the response (adhesive wear characteristics) and process parameters (load, sliding velocity and sliding distance). A relationship was built with the aid of higher order regression model as shown in equation (3):

$$Y = a + \sum a_i x_{iu} + \sum a_{ii} x_{iu}^2 + \sum a_{ij} x_{iu} x_{ju} \quad (3)$$

where 'Y' is the response, 'a' explains the effect of linearity, 'a_{ii}' explains the effect of higher order and 'a_{ij}' denotes the interaction effect. Analysis was carried out using Minitab 18. The number of parameters denotes the number of runs in an experiment in RSM. To evaluate the adhesive wear properties of hybrid MMC, a central composite design (CCD) with three numbers of continuous factors was considered.

Twenty experimental runs were generated for studying the relation between the various process parameters. The optimized process parameters for minimum wear rate will be obtained using RSM from the range of parameters considering for the analysis [15,22]. Table 2 shows the various experimental parameters and the respective levels.

Table 2. Experimental parameters and the levels.

Factors	Levels				
	1	2	3	4	5
Load (N)	10	16	25	34	40
Sliding velocity (m/s)	1	1.6	2.5	3.4	4.0
Sliding distance (m)	500	804	1250	1696	2000

3. RESULTS AND DISCUSSIONS

The adhesive wear results of AMMC obtained by varying experimental parameters are shown in Table. 3. Each experiment was conducted three times and the wear rate (average values) was calculated.

Table 3. Wear Process Parameters and its results.

S. No.	Load (N)	Sliding velocity (m/s)	Sliding distance (m)	Wear rate (mm^3/m)
1	10	2.5	1250	0.000385185
2	16	3.4	1696	0.001004542
3	16	1.6	1696	0.000436758
4	16	3.4	804	0.000644924
5	16	1.6	804	0.000414594
6	25	2.5	1250	0.000503704
7	25	2.5	1250	0.000533333
8	25	1	1250	0.001007407
9	25	2.5	1250	0.00077037
10	25	2.5	2000	0.000648148
11	25	4	1250	0.000681481
12	25	2.5	1250	0.000355556
13	25	2.5	1250	0.000651852
14	25	2.5	500	0.000518519
15	25	2.5	1250	0.000444444
16	34	1.6	1696	0.00102638
17	34	3.4	1696	0.003100978
18	34	3.4	804	0.011700755
19	34	1.6	804	0.000552792
20	40	2.5	1250	0.003111111

3.1 Influence of load on wear behaviour

The adhesive wear plots were obtained for every combination of parameters. The plot obtained for load vs velocity vs wear rate (Fig.

5) shows that wear rate increased gradually with increase in applied load (10 to 20 N) due to initial reluctance to plastic deformation, whereas with further increase in load (20 to 40 N) the sliding manner of particles over the specimen surface resulted in a cutting and ploughing condition. Rate of wear increased in a non-linear fashion from normal to severe and this increasing trend was observed for low and high velocity conditions.

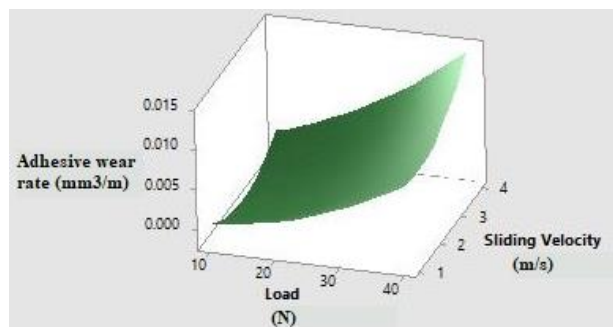
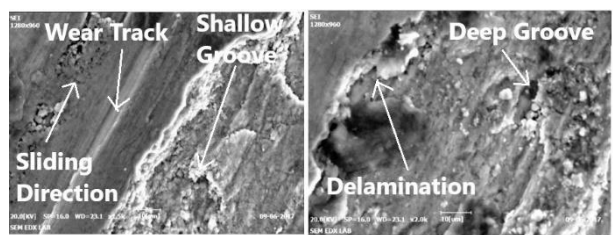


Fig. 5. Adhesive rate of wear plot in terms of load and sliding velocity for a constant sliding distance of 1250 m.



(a) L= 10N, V= 2.5m/s, SD=1250m
(b) L=40N, V=2.5 m/s, SD = 1250m

Fig. 6. Worn surface of specimen at varied loads.

The influence of experimental parameters on rate of wear was observed by analyzing the worn specimens using Scanning electron Microscopy (SEM). For a minimal load of 10N (Fig. 6a), shallow grooves with scratches and wear track along the sliding direction were observed on the specimen surface, hence minimum rate of wear was observed due to minimum surface interaction at the interface. The reinforcement particles TiO_2 acted as load bearing members, thereby limiting the amount of load transferred to the LM13 matrix [20]. At a maximum load of 40 N (Fig. 6b), the severity of wear was indicated on surface of specimen with large number of thin grooves increasing with depth. The rise in rate of wear was due to high temperature developed at the contact region resulting in a higher plastic deformation. This was followed by delamination at high temperature along the interface, resulting

in more removal of material. Hence the surface analysis at high load matches the trend observed plot of load and sliding velocity indicating an increased rate of wear with increase in load, similar inferences were observed in aluminum reinforced with alumina and graphite fabricated via liquid metallurgy route [16].

3.2 Effect of wear behavior on sliding velocity

Figure 7 showed that, initially sliding velocity decreases with rate of wear and reaching a peak value at 4 m/s. At 1 m/s the rate of wear was found to be maximum and is in correspondence with the higher period of contact with the specimen. At 2.5 m/s velocity, higher temperatures were observed at the contact region which resulted in formation of oxide layer called mechanically mixed layer (MML). This formed oxide layer acted as lubricant layer along with soft lubricant MoS_2 reinforcement and protects the specimen surface from higher wear. Similar observation was reported by another researcher in the case of AlSi10Mg alloy reinforced with (3, 6, 9 wt.%) alumina and (3 wt.%) graphite at a high velocity (3.5 m/s) [21].

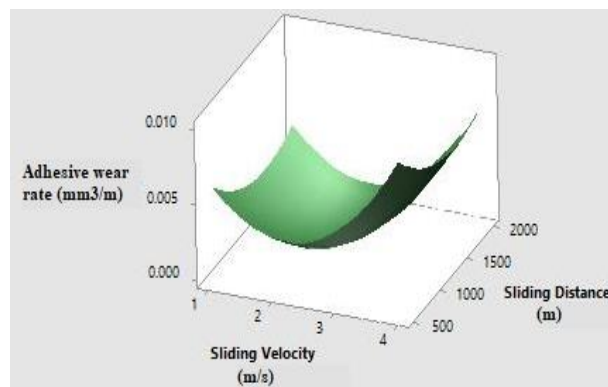


Fig. 7. Adhesive rate of wear plot in terms of sliding velocity and sliding distance for a constant load of 25 N.

The MML formation (Fig. 8a) provides a lubricating effect at the interface during the sliding, thereby decreasing the wear rate initially. Later, breakdown of MML took place where a transition towards larger rate of wear was observed. The curvatures in the trend attributed to a variation of adhesive rate of wear which was non-linear due to parameters at low and high sliding distance. The formation of MML was verified by conducting an Energy Dispersive X-ray spectroscopy (EDX) analysis where iron (12.36%) and oxygen (4.33%) was

found in significant amount (Fig. 8b and 8c), indicating the formation of oxide layers (MML) over the specimen surface[22].

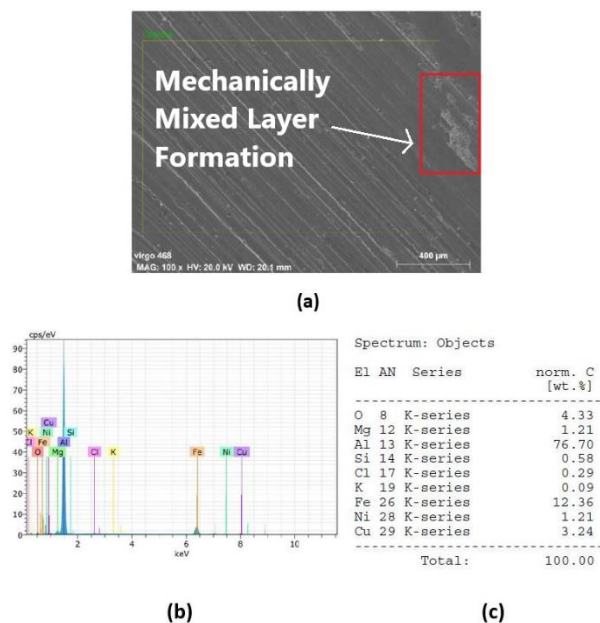


Fig. 8. (a) Formation of MML on the specimen surface, (b) Plot for energy level Vs Energy Consumption, (c) Elemental composition of specimen determined from EDX analysis.

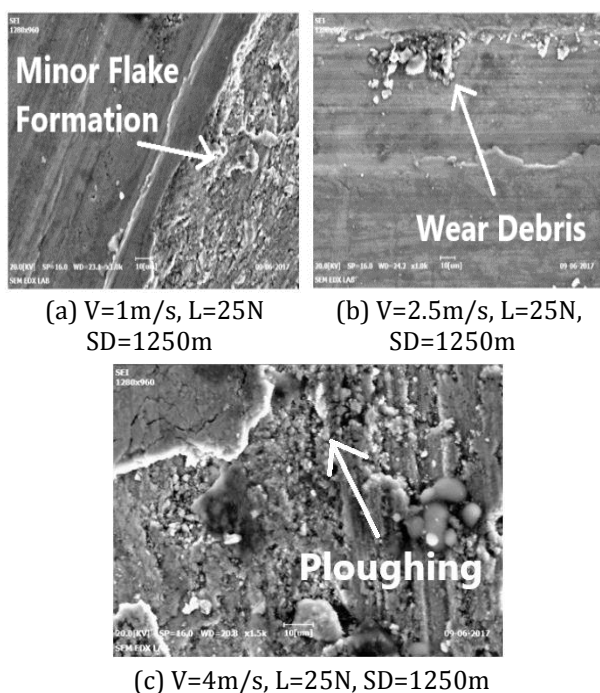


Fig. 9. Worn surface of Specimen at varied sliding velocities.

Worn surface of the composite specimens for varied sliding velocities (1-4 m/s) at constant load (25 N) and sliding distance (1250 m) were analyzed. The surface of the specimen showed

deformation along with distinctive grooves and flake formation at minimal sliding velocity (Fig. 9a). Wear was observed on the specimen at intermediate sliding velocity (2.5 m/s) which is resulted from the sliding of specimen and minimum material removal rate was observed due to the formation of MML. Whereas for a maximum velocity of 4 m/s (Fig. 9c), large number of deep grooves and extruded reinforcements were observed on the specimen surface due to ploughing action at the interface which in turn increased the material removal rate.

3.3 Influence of sliding distance on wear behavior

Figure 10 shows a trend similar to load and sliding velocity. It was observed that from this plot that, initially rate of wear increases with decreased sliding distance (500-1250 m). This attributes to the hard reinforcement particles protruded at the specimen surface which encounters the counter face at low sliding distance (500 m) and greater removal of material was observed. Eventually the increase in sliding distance up to 804 m allows the smoothing of the sharp hard protrusions resulting in uneven surface of contact. Decreased rate of wear was observed with decreased sliding distance (804-2000 m) ensuing adjacent layer of particles being exposed to the counter face resulting in larger rate of material removal.

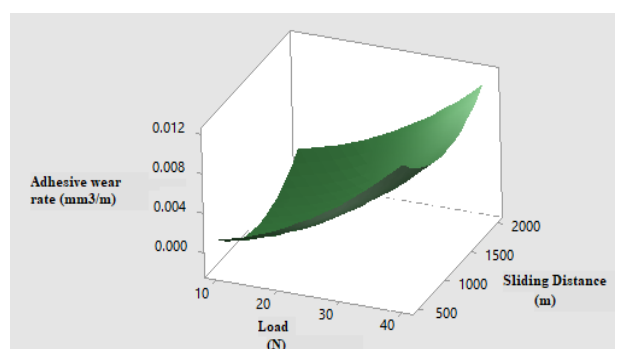
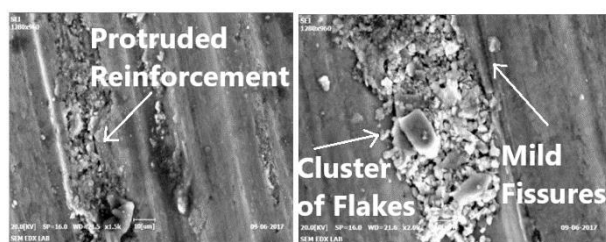


Fig. 10. Adhesive rate of wear plot in terms of load and sliding distance for a constant sliding velocity of 2.5 m/s.

In Fig. 11a, for a specific condition (minimal sliding distance of 500 m at a load of 25 N at sliding velocity of 2.5 m/s) surface of the worn specimen was observed. It is evident that, at a low sliding distance, deep cuts were formed due

to the reinforcement particles protruding out from the surface of specimen which explained the initial higher wear rate shown in surface plot (Fig. 10).



(a) SD=500m, V=2.5m/s, (b) SD=2000m, V=2.5m/s, L=25N

Fig. 11. Worn surface of specimen at varied sliding distances.

Figure 11b shows that, mild fissures and cluster of flakes occurred along the sliding direction at (2000 m) resulting in higher material removal rate. Prasat et al. observed a similar result in the case of aluminium/flyash/graphite hybrid composite, where the increase in sliding distance led to a higher rate of wear [15].

3.4 Optimization of a response

Optimizing the responses using RSM technique aids in identifying the specific parameters which leads to minimal rate of wear [23,24]. The inputs provided in the optimization process are target (0.0003556 mm³ /m), lower (10 N) and upper (40 N) bounds. The targeted wear rate was achieved at an optimum load of 11 N, sliding velocity of 1 m/s and a sliding distance of 848 m (Fig. 12).

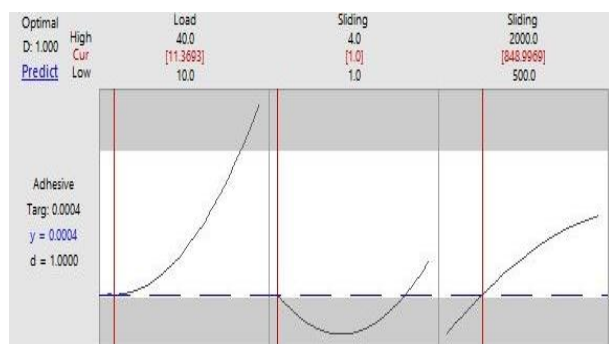


Fig. 12. Optimum values of process parameters obtained using RSM.

Figure 13 explains the optimal conditions at which worn specimen is observed. It is evident that thin flakes with minor scratches were

observed on the specimen leading to minimum removal of material.

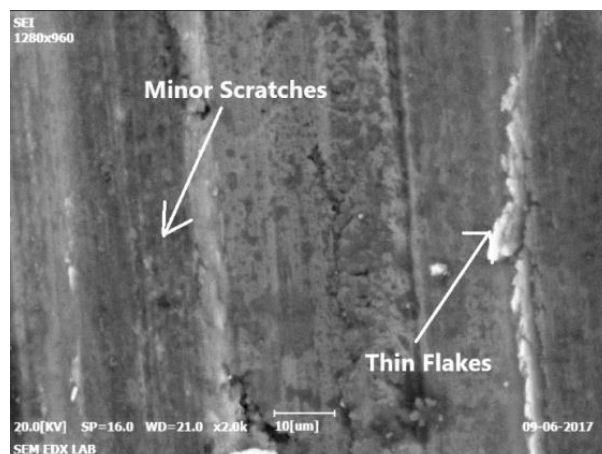


Fig. 13. Worn surface of specimen at optimum condition.

4. CONCLUSION

AMMC with MoS₂ (3%wt) and TiO₂ (12%wt) particles was synthesized via stir casting. RSM was used to generate the surface plots for different combinations of parameters.

- Results revealed that, the wear rate increases gradually as load increases and at maximum load of 40N, thin grooves with increasing depth was observed leading to severe delamination.
- In case of sliding velocity, the wear rate decreases initially due to formation of MML which acted as lubricated layer coupled with MoS₂ and then increases at higher velocities leading to the formation of deep grooves on the specimen surface due to ploughing action.
- The effect of sliding distance Vs wear rate revealed that, at low sliding distance of 500 m, the protruding reinforcement results in deep cuts on the surface of the specimen. As sliding distance increases to 2000 m, more material removal rate has been observed as the crushed reinforcements acted as third particle during the wearing process.
- Response Surface methodology was useful in identifying the process parameters at an optimized load of 11 N, sliding velocity of 1 m/s and sliding distance of 848 m for achieving minimal wear rate.
- Thus, the developed AMMC with significant wear resistance could be utilized in

Automotive applications such as piston cylinder liners where they operate under constant recursive wear and also can be used in manufacturing of aerospace parts such as bearings and gears of an aircraft engine operating at elevated temperatures and subjected to high friction.

REFERENCES

- [1] S. Das, *Development of Aluminum Alloy Composites for Engineering Applications*, Transactions-Indian Institute of Metals, vol. 57, no. 4, pp. 325-334, 2004.
- [2] P. Cichosz, P. Karolczak, *Sinker Electric Discharge Machining of Aluminum Matrix Composites*, Material Science-Poland, vol. 26, no. 3, pp. 547-554, 2008.
- [3] S. Marichamy, M. Saravanan, M. Ravichandran, G. Veerappan, *Parametric Optimization of Electrical Discharge Machining Process On a α - β Brass Using Grey Relational Analysis*, Journal of Materials Research, vol. 31, iss.16, pp. 2531-2537, 2016, doi: [10.1557/jmr.2016.213](https://doi.org/10.1557/jmr.2016.213)
- [4] S.J. James, K. Venkatesan, P. Kuppan, R. Ramanujam, *Hybrid Aluminum Metal Matrix Composite Reinforced with SiC and TiB₂*, Procedia Engineering, vol. 97, pp. 1018-1026, 2014, doi: [10.1016/j.proeng.2014.12.379](https://doi.org/10.1016/j.proeng.2014.12.379)
- [5] A.H. Idrisi, S. Deva, *Development and Testing of Metal Matrix Composite by Reinforcement of SiC Particles on Al 5XXX Series Alloy*, International Journal of Science Engineering Research, vol. 3, iss. 2, pp. 1303-1309, 2014.
- [6] S. Daniel, G. Harish, *A Study on the Behavior of Aluminum Alloy (LM13) Reinforced with Nano ZrO₂ particulate*, IOSR Journal of Engineering, vol. 4, iss. 2, pp. 58-62, 2014.
- [7] K.S. Vinoth, R. Subramanian, S. Dharmalingam, B. Anandavel, *Mechanical and Tribological Characteristics of Stir Cast Al-Si10Mg and Self-lubricating Al-Si10mg/MoS₂ Composites*, Materials and technology, vol. 46, no. 5, pp. 497-501, 2012.
- [8] J.D.R. Selvam, D.S.R. Smart, I. Dinaharan, *Synthesis and Characterization of Al-6061-FlyAsh-SiC Particulate Composites by Stir Casting and Compo Casting*, Energy Procedia, vol. 34, pp. 637-646, 2013, doi: [10.1016/j.egypro.2013.06.795](https://doi.org/10.1016/j.egypro.2013.06.795)
- [9] T. Hariprasad, K. Varatharajan, S. Ravi, *Wear Characteristics of B₄C and Al₂O₃ Reinforced with Al 5083 Metal Matrix Based Hybrid Composite*, Procedia Engineering, vol. 97, pp. 925-929, 2014, doi: [10.1016/j.proeng.2014.12.368](https://doi.org/10.1016/j.proeng.2014.12.368)
- [10] S.C. Sharma, *The Sliding Wear Behavior of Al 6061- Garnet Particulate Composite*, Wear, vol. 249, iss. 12, pp. 1036-1045, 2001, doi: [10.1016/S0043-1648\(01\)00810-9](https://doi.org/10.1016/S0043-1648(01)00810-9)
- [11] M. Demirel, M. Muratoglu, *Influence of Load and Temperature on the Dry Sliding Wear Behavior of Aluminum- Ni₃Al Composites*, Indian Journal of Engineering & Material Science, vol. 18, pp. 268-282, 2011.
- [12] M. Asif, K. Chandra, P.S. Misra, *Development of Aluminum Based Hybrid Metal Matrix Composites for Heavy Duty Applications*, Journal of Mineral & Material Characteristic & Engineering, vol. 10, no. 14, pp. 1337-1344, 2011.
- [13] N. Sharma, R. Khanna, G. Singh, V. Kumar, *Fabrication of 6061 Aluminum Alloy Reinforced with Si₃N₄/n-Gr and its Wear Performance Optimization Using Integrated RSM-GA*, Particulate Science and Technology, vol. 35, iss. 6, pp. 731-741, 2017, doi: [10.1080/02726351.2016.1196276](https://doi.org/10.1080/02726351.2016.1196276)
- [14] M. Bayhan, K. Onel, *Optimization of Reinforcement Content and Sliding Distance for AlSi7-Mg/SiCp Composites Using Response Surface Methodology*, Material & Design, vol. 31, iss6, pp. 3015-3022, 2010, doi: [10.1016/j.matdes.2009.12.049](https://doi.org/10.1016/j.matdes.2009.12.049)
- [15] S.V. Prasat, R. Subramanian, N. Radhika, B. Anandavel, *Dry Sliding Wear and Friction Studies on AlSi10Mg-Flyash-Graphite Hybrid Metal Matrix Composites Using Taguchi Method*, Tribology-Materials, Surfaces & Interfaces, vol. 5, iss. 2, pp. 72-81, 2011, doi: [10.1179/1751584X11Y.0000000009](https://doi.org/10.1179/1751584X11Y.0000000009)
- [16] N. Radhika, R. Subramanian, *Wear Behavior of Aluminum/ Alumina/Graphite Hybrid Metal Matrix Composite Using Taguchi's Techniques*, Industrial Lubrication and Tribology, vol. 65, no. 3, pp. 166-174, 2013, doi: [10.1108/00368791311311169](https://doi.org/10.1108/00368791311311169)
- [17] S. Ankush, Ram Narayan, R.D. Gupta, *Evaluation and Comparison of Mechanical Properties of Aluminum Alloy 5052 Reinforced with Silicon Carbide, Graphite and Fly ash Hybrid Metal Matrix Composites*, International Journal of Engineering Science and Technology, vol. 5, pp. 1780-1787, 2013.
- [18] K. Kanthavel, K.R. Sumesh, P. Saravanakumar, *Study of Tribological Properties on Al/Al₂O₃/MoS₂ Hybrid Composite Processed by Powder Metallurgy*, Alexandria Engineering Journal, vol. 55, iss. 1, pp. 13-17, 2016, doi: [10.1016/j.aej.2016.01.024](https://doi.org/10.1016/j.aej.2016.01.024)
- [19] S.C. Vetrivel, N. Selvakumar, R. Narayanasamy, N. Leema, *Numerical Modelling, Prediction of Cu-W Nano Powder Composite in Dry Sliding Wear Condition Using Response Surface Methodolgy*, Material & Design, vol. 50, pp. 977-996, 2013, doi: [10.1016/j.matdes.2013.03.072](https://doi.org/10.1016/j.matdes.2013.03.072)

- [20] G. Elango, B.K. Ragnath, *Tribological Behavior of Hybrid (LM25Al+SiC+TiO₂) Metal Matrix Composites*, Procedia Engineering, vol. 64, pp. 671-680, 2013, doi: [10.1016/j.proeng.2013.09.142](https://doi.org/10.1016/j.proeng.2013.09.142)
- [21] N. Radhika, R. Subramanian, *Effect of Reinforcement on Wear Behavior of Aluminum Hybrid Composites*, Tribology-Materials, Surfaces & Interfaces, vol. 7, iss. 1, pp. 36-41, 2013, doi: [10.1179/1751584X13Y.0000000025](https://doi.org/10.1179/1751584X13Y.0000000025)
- [22] R. Jojith, N. Radhika, *Mechanical and Tribological properties of LM13/TiO₂/MoS₂ Hybrid Metal Matrix Composite Synthesized by Stir Casting*, Particulate Science and Technology, vol. 37, iss. 5, pp. 566-578, 2019, doi: [10.1080/02726351.2017.1407381](https://doi.org/10.1080/02726351.2017.1407381)
- [23] A. Nayak, D.K. Jesthi, B.C. Routara, D. Das, R.K. Nayak, *Tribological properties of glass/carbon hybrid composites through inter-ply arrangement using Response Surface Methodology*, Materials Today Proceedings, vol. 5, iss. 9, pp. 19828-19835, 2018, doi: [10.1016/j.matpr.2018.06.346](https://doi.org/10.1016/j.matpr.2018.06.346)
- [24] H. Joardar, *Optimization for Turning of Aluminium and Titanium Di Boride Cast Composites Using Response Surface Methodology*, Materials Today Proceedings, vol. 5, iss. 11, pp. 23576-23585, 2018, doi: [10.1016/j.matpr.2018.10.146](https://doi.org/10.1016/j.matpr.2018.10.146)